Journal of the European Ceramic Society 22 (2002) 2933–2937

www.elsevier.com/locate/jeurceramsoc

Subsolidus relations in the $BaO–La_2O_3–V_2O_5$ phase diagram

M.G. Skellern, J.M.S. Skakle*

Department of Chemistry, University of Aberdeen, Aberdeen AB24 3UE, UK

Received 15 November 2001; received in revised form 6 February 2002; accepted 24 February 2002

Abstract

The subsolidus region of the $BaO–La_2O_3–V_2O_5$ phase diagram has been redetermined. Previously reported binary phases of $LaVO_4$, $La_8V_2O_{17}$, La_3VO_7, $BaLa_2O_4$, $Ba_3V_2O_8$, $Ba_2V_2O_7$, $Ba_3V_4O_{13}$ and BaV_2O_6 have all been confirmed. The ternary phases $Ba_2LaV_3O_{11}$, $Ba_3LaV_3O_{12}$ and $Ba_3La_{40}V_{12}O_{93}$ have also been confirmed. The new phase "$BaLa_{10}V_4O_{26}$" has been synthesised for the first time and is reported here along with the amended phase diagram. The previously omitted phase of $La_{1.42}V_{0.58}O_{3.58}$ has also been included and reasons for this are cited. The diagram is shown for two temperatures (1000 and 600 °C) due to the low melting point of V_2O_5-rich compounds. © 2002 Elsevier Science Ltd. All rights reserved.

Keywords: Electron microscopy; Phase diagram; Powders–solid state reaction; Transition metal oxides; X-ray methods; $BaO–La_2O_3–V_2O_5$

1. Introduction

There has been much research into new and effective luminescent materials based on oxides of vanadium, the alkaline earth elements and the lanthanides.[1] Such materials are extensively used in lasers, in phosphors (luminescent materials), for display screen equipment and in electric lighting. Despite this, the phase relationships in the ternary system $MO–Ln_2O_3–V_2^VO_5$ (M = Ba, Ca, Sr; Ln = lanthanide) have not been widely studied.

The $BaO–La_2O_3–V_2O_5$ system is of interest for two reasons. First, as it is a member of the aforementioned group, there may be phases within this system which display interesting luminescent, relaxation or energy transfer phenomena. Secondly, the previously reported $M_{3-3x}La_{2x}V_2O_8$ solid solutions (M = Ba,Sr)[2,3,4] display ionic conductivity over a wide range of temperatures and pressures and may also display electronic conductivity.[2,3] This latter property occurs at low oxygen partial pressures, such that $V^V \rightarrow V^{IV} + e^-$. There is a great deal of interest in ionic conductors due to the array of practical applications in which these materials may be exploited, and these materials are thus the subject of a patent.[5] Therefore, an appreciation of the entire phase diagram is of benefit.

A number of binary phases in the system have been reported. Along the $BaO–V_2O_5$ binary system lies BaV_2O_6,[6] $Ba_3V_4O_{13}$,[7,8] $Ba_2V_2O_7$[9,10] and $Ba_3V_2O_8$.[6,11] Four lanthanum vanadates are formed in $La_2O_3–V_2O_5$ system, namely the orthovanadate $LaVO_4$,[12,13] $La_{1.42}V_{0.58}O_{3.58}$,[11] $La_8V_2O_{17}$[11,12] and La_3VO_7.[11,12] LaV_3O_9 has also been reported but was synthesised hydrothermally,[14] so is not included in the equilibrium phase diagram. The $BaO–La_2O_3$ system contains only $BaLa_2O_4$.[15]

$Ba_3V_2O_8$ displays the palmierite structure and is the end-member of a pseudo-binary system, $Ba_3V_2O_8–LaVO_4$, where $Ba_3LaV_3O_{12}$ has been reported as the limiting composition.[4] Two complex oxovanadates are formed; $Ba_2LaV_3O_{11}$ which occurs on the $Ba_2V_2O_7–LaVO_4$ tie-line and $Ba_3La_{40}V_{12}O_{93}$ which lies on the $Ba_3V_2O_8–La_8V_2O_{17}$ tie-line.[16] The phase diagram has been reported previously with these three ternary phases identified[15]. However, during synthesis of the $Ba_{3-3x}La_{2x}V_2O_8$ solid solution, new ternary phases were identified as second phases indicating that the phase diagram was incomplete; a redetermination of the subsolidus relations of $BaO–La_2O_3–V_2O_5$ was therefore deemed necessary.

2. Experimental

Starting materials were $BaCO_3$, La_2O_3 (both 99%, BDH Chemicals Ltd., Poole, UK) and V_2O_5 (99.2%

* Corresponding author. Tel.: +44-1224-272916.
E-mail addresses: j.skakle@abdn.ac.uk (J.M.S. Skakle), m.g.skellern@abdn.ac.uk (M.G. Skellern).

PII: S0955-2219(02)00048-1

Johnson Matthey, Royston, UK). La_2O_3 was dried at 900 °C prior to use; $BaCO_3$ and V_2O_5 were both dried at 300 °C. Appropriate quantities of starting materials were ground in an agate mortar and pestle under acetone, then pressed into 13 mm diameter pellets. The pellets were placed on platinum foil and heated between 650–1200 °C with intermediate grindings for a period of 3–7 days. Powder X-ray diffraction was performed using a Bruker D8 Advance with twin Göbel mirrors, CuK_α radiation and phase identification was achieved

Table 1
Key compositions synthesised and resultant phases formed in the $BaO–La_2O_3–V_2O_5$ system

Sample identification	Composition (%)	Sintering temperature (°C)	No. of phases	Phases present	Area in Fig. 1
K	50%Ba; 30%La; 20%V	1000	3	BaO $Ba_3V_2O_8$ $BaLa_2O_4$	1
A 21 23	40%Ba; 40%La; 20%V 50%Ba; 20%La; 30%V 20%Ba; 70%La; 10%V	1110	3	$BaLa_2O_4$ $Ba_3V_2O_8$ La_2O_3	2
17	30%Ba; 50%La; 20%V	1100	2	La_2O_3 $Ba_3V_2O_8$	Tie-line
M	20%Ba; 60%La; 20%V	1100	3	$Ba_3V_2O_8$ La_2O_3 $Ba_3La_{40}V_{12}O_{93}$	3
F C	20%Ba; 40%La; 40%V 0%Ba; 50%La; 40%V	1050	3	$Ba_3LaV_3O_{12}$ $LaVO_4$ $BaLa_{10}V_4O_{26}$	4
I	30%Ba; 23%La; 47%V	1100	3	$Ba_3LaV_3O_{12}$ $Ba_2LaV_3O_{11}$ $LaVO_4$	5
D	20%Ba; 30%La; 50%V	1100	2	$Ba_2LaV_3O_{11}$ $LaVO_4$	Tie-line
N	10%Ba; 37%La; 53%V	900	3	$Ba_2LaV_3O_{11}$ BaV_2O_6 $LaVO_4$	6
P B	36%Ba; 30%La; 34%V 30%Ba; 40%La; 30%V	1075	2	$Ba_{3-3x}La_{2x}V_2O_8$ $Ba_3La_{40}V_{12}O_{93}$	8
E	44.44%Ba; 11.12%La; 44.44%V	1150	2	$Ba_{3-3x}La_{2x}V_2O_8$ $Ba_2LaV_3O_{11}$	9
H	2%Ba; 71%La; 26%V	1100	3	$BaLa_{10}V_4O_{26}$ $LaVO_4$ $La_{1.42}V_{0.58}O_{3.58}$	10
Q	10%Ba; 64%La; 26%V	750	3	$Ba_3La_{40}V_{12}O_{93}$ $Ba_3LaV_3O_{12}$ $BaLa_{10}V_4O_{26}$	11
S	3% Ba; 71% La; 26%V	1100	3	$La_{1.42}V_{0.58}O_{3.58}$ $BaLa_{10}V_4O_{26}$ $Ba_3La_{40}V_{12}O_{93}$	12
T	2% Ba; 81% La; 17%V	1100	3	$La_8V_2O_{17}$ $Ba_3La_{40}V_{12}O_{93}$ La_2O_3	13
U	2% Ba; 76% La; 22%V	1100	3	La_3VO_7 $Ba_3La_{40}V_{12}O_{93}$ $La_8V_2O_{17}$	14

using Bruker "Eva" search/match software[17] and the ICDD powder diffraction file.[18] In addition, quantitative electron-probe microanalysis (EPMA) was performed using a Cameca SX51 EPMA, with standards $BaSO_4$ for Ba L_α, LaB_6 for La L_α, V_2O_5 for V K_α. Samples were embedded in epoxy resin, polished to >1 μm and coated with carbon. A beam voltage of 20 kV and a beam current of 50 nA was used for the analysis. For each sample, around 20 points were analysed and the results averaged.

3. Results and discussion

The results of the phase diagram study are presented in Table 1, which gives a summary of the main compositions prepared, the synthesis conditions and the resultant phases present, as determined by XRD and EPMA. These results led to the construction of the phase diagram as shown in Fig. 1. The phase diagram is presented with end members BaO, $1/2(La_2O_3)$ and $1/2(V_2O_5)$ so that compositions are a simple ratio of the metals, Ba:La:V.

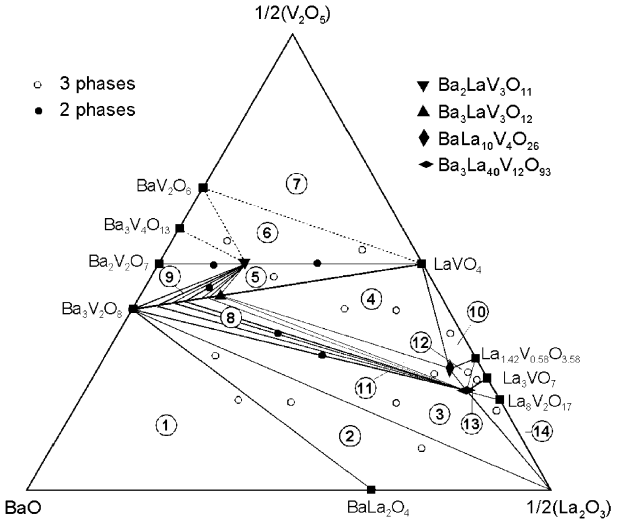

Fig. 1. Subsolidus relations in the $BaO–La_2O_3–V_2O_5$ phase diagram, showing key compositions synthesised. The diagram is shown for 2 temperatures: 1000 °C (solid lines) and 600 °C (solid plus dashed lines).

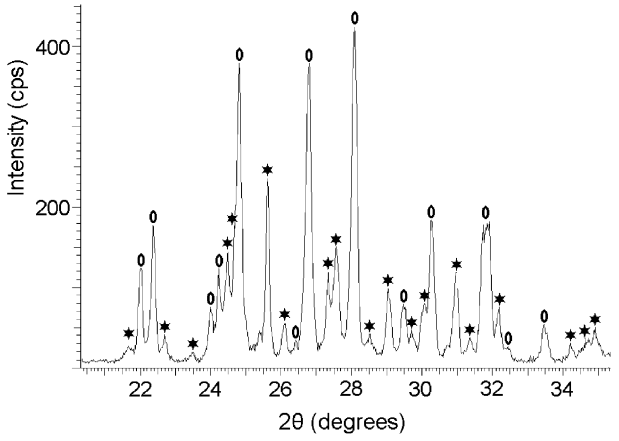

Fig. 2. Powder X-ray diffration pattern for the composition "$Ba_4LaV_5O_{18}$", showing that it is a mixture of $Ba_2V_2O_7$ (⋆) and $Ba_2LaV_3O_{11}$ (**0**).

The compatability triangle $Ba_3V_2O_8–BaLa_2O_4–BaO$ was deduced from sample K (50%Ba: 30%La: 20%V); a sample of higher BaO content, (70%Ba: 15%La: 15%V) was synthesised at 900 °C but melted. Similarly, for samples of high V_2O_5 content, melting temperatures were low, and thus the phase diagram is shown for two temperatures. At 1000 °C, only samples of 50% V and below were stable (solid lines), whereas at 600 °C, compositions up to 67% V were stable (solid + dashed lines). The phase $Ba_4LaV_5O_{18}$ was first identified by EPMA as a minor phase while analyzing a sample close in composition on the phase diagram. A sample of this stoichiometry was synthesised but the XRD pattern revealed it to comprise of two phases, $Ba_2V_2O_7$ and $Ba_2LaV_3O_{11}$ (Fig. 2). Subsequant EPMA of this composition confirmed this result, thus agreeing with the tie-line previously reported by Serkalo et al.[16]

A composition near $BaLa_{10}V_4O_{26}$ was firstly detected by EPMA as a minor phase and was then synthesised. EPMA results are given in Table 2a and in Fig. 3. Accurate analysis was problematic due to small grain sizes, even after extended sintering periods, but the EPMA results would give a stoichiometric formula of $Ba_2La_{21}V_8O_{53.5}$. The oxygen content given in Table 2a was calculated by difference and may be unreliable due to the porosity of the sample. Thus, the oxygen content given here is calculated from stoichiometry assuming V^V. In addition the overall analysis is subject to larger errors than normal due to the porosity of the sample

Table 2
EPMA results for (a) $BaLa_{10}V_4O_{26}$ and (b) $Ba_2LaV_3O_{11}$

	Concentration (wt .%)		At. %	
	Average	Standard deviation	Average	Standard deviation
(*a*)				
Ba	6.048	0.123	2.345	0.042
La	64.462	0.327	24.715	0.110
V	9.158	0.107	9.578	0.075
O	19.035	0.114	63.362	0.031
Total	98.703		100.00	
(*b*)				
Ba	36.93	0.16	11.91	0.05
La	18.49	0.15	5.90	0.06
V	20.18	0.11	17.55	0.05
O	23.35	0.08	64.64	0.03
Total	98.95		100.00	

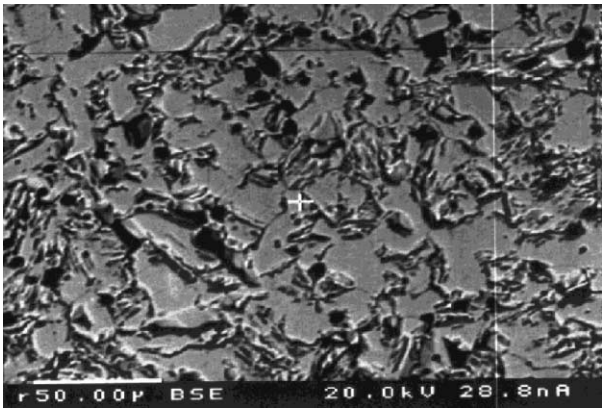

Fig. 3. EPMA analysis of "$BaLa_{10}V_4O_{26}$": backscattered electron image, showing small grain size and porosity of single phase sample.

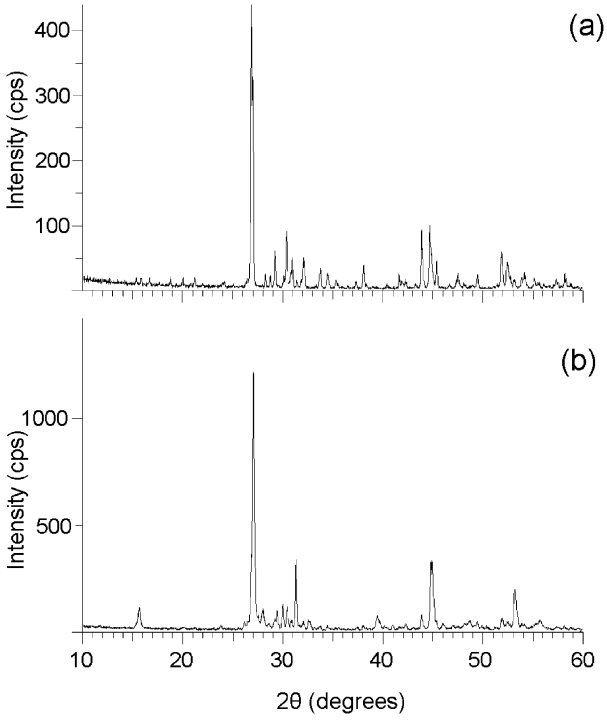

Fig. 4. Powder X-ray diffraction patterns for (a) $BaLa_{10}V_4O_{26}$ and (b) $Ba_3La_{40}V_{12}O_{93}$.

and thus the simpler stoichiometry of $BaLa_{10}V_4O_{26,}$ as was used for synthesis, is retained for the phase diagram. The stoichiometry of $BaLa_{10}V_4O_{26}$ is very close to that of $Ba_3La_{40}V_{12}O_{93}$ but produces a unique XRD pattern (Fig. 4) and therefore is a distinct phase. Powder X-ray diffraction data for $BaLa_{10}V_4O_{26}$ is given in Table 3.

The inclusion of $La_{1.42}V_{0.58}O_{3.58}$ is necessary. This sample had been omitted from the earlier phase diagram based on the fact that it is non-stoichiometric. It is not, however, part of a solid-solution, gives a unique XRD pattern and is phase pure as deducted by EPMA; thus, as it is stable at the appropriate temperature for this phase diagram, it should be included.

Table 3
Powder X-ray diffraction data for $BaLa_{10}V_4O_{26}$

d /Å (10^{-10}m)	2θ /°	I/I_{max}
4.73631	18.720	4.0
4.43551	20.002	3.6
4.19590	21.157	3.9
3.68481	24.133	2.9
3.32727	26.772	100.0
3.30809	26.930	68.0
3.16161	28.203	4.7
3.10894	28.691	4.9
3.05887	29.171	13.1
2.97071	30.057	4.8
2.94311	30.345	21.5
2.90276	30.778	6.3
2.88935	30.924	11.1
2.84487	31.420	3.4
2.81006	31.819	4.0
2.79354	32.013	9.7
2.78275	32.140	8.9
2.65476	33.735	6.8
2.59873	34.485	5.4
2.54114	35.292	3.2
2.40780	37.316	3.1
2.36261	38.057	8.8
2.16734	41.637	6.1
2.15364	41.915	3.3
2.13686	42.260	3.6
2.09049	43.244	2.6
2.06078	43.899	22.1
2.02552	44.704	25.0
2.01594	44.928	11.0
1.99812	45.351	10.8
1.91840	47.348	4.0
1.84224	49.434	5.5
1.76256	51.830	12.6
1.74380	52.429	10.2
1.73385	52.753	4.7
1.72195	53.147	3.6
1.70002	53.887	4.7
1.69226	54.154	6.6
1.66216	55.218	4.0
1.60329	57.429	4.3
1.58249	58.256	6.3

$La_{1.62}V_{0.38}O_{3.38}$ (81% La:19% V), reported by Kitayama et al,[11] was synthesised and has an identical XRD pattern to that of $La_8V_2O_{17}$. There are two possibilities: first, that $La_8V_2O_{17}$ forms a small but identifiable solid solution, or second, that $La_{1.62}V_{0.38}O_{3.38}$ actually consists of a mixture of $La_8V_2O_{17}$ and La_2O_3. If the latter were the case then La_2O_3 would be present in small enough quantities so as not to be detectable by XRD. Even by EPMA it may be either undetectable or fall within expected limits of error for synthesis. Therefore, in this report, only $La_8V_2O_{17}$ is marked on the phase diagram.

Quantitative EPMA analysis was also performed on a sample of $Ba_2LaV_3O_{11}$; oxygen content was not determined directly but calculated by stoichiometry for each point analysed, again assuming fixed valence for

each cation and V^V. The results revealed a single phase sample of stoichiometry $Ba_{2.02(1)}La_{1.00(1)}V_{2.97(1)}O_{10.96(1)}$ thus confirming the previously reported phase $Ba_2LaV_3O_{11}$.

4. Conclusions

Two phases have been added to the $BaO–La_2O_3–V_2O_5$ phase diagram. $La_{1.42}V_{0.58}O_{3.58}$ has been reported previously but was not included in the original phase diagram. In addition, a new ternary phase has been identified of approximate composition $BaLa_{10}V_4O_{26}$. This is close in composition but distinct from the previously reported phase $Ba_3La_{40}V_{12}O_{93}$.

As a result of the addition of $La_{1.42}V_{0.58}O_{3.58}$ and $BaLa_{10}V_4O_{26}$, the subsolidus region of the phase diagram has changed from the earlier determination.[12] The presence of the following new compatibility triangles was confirmed by XRD: $Ba_3LaV_3O_{12}–BaLa_{10}V_4O_{26}–Ba_3La_{40}V_{12}O_{93}$ (Area 11, Fig. 1), $BaLa_{10}V_4O_{26}$-$La_{1.42}V_{0.58}O_{3.58}$-$Ba_3La_{40}V_{12}O_{93}$ (Area 12, Fig. 1) and $Ba_3La_{40}V_{12}O_{93}$-$La_{1.42}V_{0.58}O_{3.58}$-$La_3VO_7$ (Area 13, Fig. 1)

Acknowledgements

We would like to thank the University of Aberdeen (MGS) and EPSRC for funding. We also acknowledge the use of the EPSRC's Chemical Data-base Service at Daresbury.[18]

References

1. Fotiev, A. A., Shul'gin, B. V., Moskvin, A. S. and Gavrilov, F. F., *Vandium Crystal-phosphors, Izd.* Nauka, Moscow, 1976.
2. Leonidov, I. A., Leonidova, O. N. and Fotiev, A., Electrotransport in solid solutions $M_{3-3x}La_{2x}O_x(VO_4)_2$ where M = Sr,Ba. *Elektrokhimya*, 1992, **28**, 1515–1522.
3. Leonidov, I. A., Leonidova, O. N. and Slepukhin, V. K., Electronic conductivity of $Sr_{3-3x}La_{2x}(VO_4)_2$ solid solutions. *Inorg. Mater. (Engl. Trans.)*, 2000, **36**, 72–75.
4. Skakle, J. M. S., Coats, A. M. and Marr, J., The crystal structures of $Ba_2R_{2/3}V_2O_8$ (R = La, Nd) and $Sr_2La_{2/3}V_2O_8$; palmierite derivatives. *J. Mater. Chem.*, 2000, **35**, 3251–3256.
5. Fukushima, S., Tanaka, S., Nibu, H., Ando, T., Takeno, S. and Nakamura, S. Electrically conductive oxides having layer perovskite structures. Jpn. Kokai Tokkyo Koho JP0504,819 [93,04,819]. JP Appl. 90/246,749.
6. Fotiev, A. A., Makarov, V. V., Volkov, V. L. and Surat, L. L., The $BaO–V_2O_5$ System. *Russ. J. Inorg. Chem. (Engl. Transl.)*, 1969, **14**, 144.
7. Gatehouse, B. M., Guddat, L. W. and Roth, R. S., The crystal structure of $Ba_3V_4O_{13}$. *J. Solid State Chem.*, 1987, **71**, 390–395.
8. Hawthorne, F. C. and Calvo, C., The crystal structure of $Ba_2V_2O_7$. *J. Solid State Chem.*, 1978, **26**, 345–355.
9. Kohlmuller, R. and Perraud, J., Équilibres liquides–solides dans les systèmes V_2O_5–BaO et V_2O_5–MgO. *Bull. Soc. Chim. France.*, 642.
10. Süsse, P. and Buerger, J., The structure of $Ba_3(VO_4)_2$. *Z. Kristallogr., Bd.*, 1970, **131**(S), 161–174.
11. Kitayama, K., Zoshima, D. and Katsura, T., Phase equilibrium in the $La_2O_3–V_2O_3–V_2O_5$ system at 1200 °C. *Bull. Chem. Soc. Jpn.*, 1983, **56**, 689–694.
12. Fotiev, V. A. and Bazuev, G. V., Phase relationships in the $La_2O_3–V_2O_5–SrO$ system. *Russ. J. Inorg. Chem.*, 1984, **29**, 1337–1340.
13. Oka, Y., Yao, T. and Yamamoto, N., Hydrothermal synthesis of lanthanum vanadates: synthesis and crystal structures of zircon-type $LaVO_4$ and a new compound LaV_3O_9. *J. Solid State Chem.*, 2000, **152**, 486–491.
14. Wong-Ng, W., Paretzkin, B. and Fuller, E. R., Crystal chemistry and phase-equilibria studies of the $BaO(BaCO_3)–R_2O_3–CuO$ systems; crystal chemistry and subsolidus phase relationship studies of the CuO-rich region of the ternary diagrams, R = Lanthanides. *J. Solid State Chem.*, 1990, **85**, 117–132.
15. Serkalo, A. A., Fotiev, V. A., Khodos, M.Ya., Bazuev, G. V. and Fotiev, A. A., Phase relationships in the $BaO–La_2O_3–V_2O_5$ system. *Russ. J. Inorg. Chem.*, 1986, **31**, 1529–1531.
16. Eva, Powder X-ray Diffraction Evaluation Program, Version 5.0 rev. 3. Bruker Analytical X-ray Systems, GmbH Karlsruhe, Germany.
17. The Powder Diffraction File, International Centre for Diffraction Data, Newtown Square, Pennsylvania, USA.
18. Fletcher, D. A., McMeeking, R. F. and Parkin, D., The United Kingdom chemical database service. *J. Chem. Inf. Comput. Sci.*, 1996, **36**, 746–749.